

# Synthesis and photochemical properties of two ICT compounds with naphthalimide and diarylamine units

Jiang Wei Tang Jinan Sun Yueming Xu Wenlian Wang Hualin

(School of Chemistry and Chemical Engineering, Southeast University, Nanjing 211189, China)

**Abstract:** Two new diarylamine-substituted 1, 8-naphthalimide derivatives are synthesized by  $\text{CuI}/18\text{-crown-6}/\text{K}_2\text{CO}_3$  catalyst system and characterized by Fourier transform infrared (FT-IR),  $^1\text{H-NMR}$  and elemental analyses. The UV-vis absorption and photoluminescent (PL) spectra of the systems in *n*-hexane, tetrahydrofuran (THF), and  $\text{CH}_2\text{Cl}_2$  are investigated. These naphthalimide molecules have an absorption band centered at about 450 nm, which is assigned to an intramolecular charge-transfer (ICT) transition, and they emit light at 492, 501 nm in a nonpolar solvent such as *n*-hexane, and at 600, 620 nm in a polar solvent such as  $\text{CH}_2\text{Cl}_2$ . From the Lippert-Mataga equation, the difference of the dipole moment between the excited state and the ground state is estimated to be 9.2 and 9.8 D for 4-(diphenylamine)-N-(2-methoxyphenyl)-1, 8-naphthalimide (DMN-1) and 4-(2-naphthylphenylamine)-N-(2-methoxyphenyl)-1, 8-naphthalimide (DMN-2), respectively. This large change in the dipole moment upon excitation is typical for photoinduced ICT processes.

**Key words:** naphthalimide; diarylamine; photoluminescence; UV-vis spectrum; intramolecular charge transfer

Naphthalimides comprise a class of chromophores whose electronic absorptions and emissions depend on the properties of the surrounding medium. The photophysical behavior of 1, 8-naphthalimide derivatives is a function of C-4 substitution<sup>[1]</sup>. Substitution of electron-donating groups usually increases fluorescence emissions, particularly when a methoxy or an amino group at C-4 position is used. Thus, they have a wide range of applications such as organic dyes and luminophores<sup>[2-4]</sup>, probes for analytical purpose<sup>[5]</sup>, fluorophores for optical chemosensing and liquid crystal displays<sup>[6-9]</sup>.

It is well known that 1, 8-naphthalimides with electron-donating groups at the C-4 position have high fluorescent quantum yields, and their emissions can be tuned easily to longer wavelengths<sup>[10]</sup>. Based on these findings, the diarylamine-substituted naphthalimides are made available by Ullmann reaction, and the absorption and photoluminescent spectra of these derivatives in *n*-hexane, THF,  $\text{CH}_2\text{Cl}_2$  are recorded to study their spectral properties under various solvent polarities and to compare their emissions. A large Stokes shift in these ICT compounds is observed in polar solvents.

Received 2007-10-29.

**Biographies:** Jiang Wei (1980—), male, graduate; Sun Yueming (corresponding author), male, doctor, professor, sun@seu.edu.cn.

**Foundation items:** The Ph. D. Programs Foundation of Ministry of Education of China (No. 20030286012), the High Technology Research and Development Program of Jiangsu Province (No. BG2005034).

**Citation:** Jiang Wei, Tang Jinan, Sun Yueming, et al. Synthesis and photochemical properties of two ICT compounds with naphthalimide and diarylamine units[J]. Journal of Southeast University (English Edition), 2008, 24 (2): 243 – 246.

## 1 Experimental

### 1.1 General

Melting points are determined on a digital melting point apparatus WRS-1 made in Shanghai and uncorrected. IR spectra are recorded on a 5DX-FT-2 spectrophotometer using KBr pellets.  $^1\text{H-NMR}$  and  $^{13}\text{C-NMR}$  spectra are recorded on a Bruker (ARX-300) spectrophotometer (300 MHz) in  $\text{CDCl}_3$  and using TMS as internal standard (Chemical shifts are given as  $\delta$  in ppm). The mass spectra are recorded on a ZAB-H spectrometer. Elemental analyses are performed on an Elementar Vario MICRO. UV-vis absorption spectra are recorded using a Hitachi U-300 spectrophotometer, while photoluminescent spectra are recorded using a Hitachi F-4050. All reactions are monitored by thin-layer chromatography. Common reagent grade chemicals are commercially available and are used without further purification.

### 1.2 Synthesis

A mixture of 4-bromo-N-(2-methoxyphenyl)-1, 8-naphthalimide (1.0 mmol), diarylamine (1.2 mmol), potassium carbonate (2.0 mmol), copper (I) iodide (0.05 mmol), 18-crown-6 (0.05 mmol) and 3 mL *o*-dichlorobenzene is heated at 190 °C for 24 to 30 h under nitrogen. After cooling, chloroform and water are added into the mixture. The organic layer is washed successively with a water and brine solution and dried over anhydrous magnesium sulfate. The crude solid is further purified by silica gel column using a petroleum ether/ethyl acetate mixture as the eluent, which gives the desired pure product.

1) 4-(diphenylamine)-N-(2-methoxyphenyl)-1, 8-naphthalimide DMN-1

Mp: 184 to 185 °C; IR (KBr,  $\text{cm}^{-1}$ ): 3 024, 1 699, 1 657, 1 271, 1 234, 754;  $^1\text{H-NMR}$  (300 MHz,  $\text{CDCl}_3$ , TMS,  $\delta$ ): 8.60 (t, 2H), 8.26 (d,  $J = 8.5$  Hz, 1H), 7.56 to 7.47 (m, 1H), 7.43 (d,  $J = 7.6$  Hz, 2H), 7.32 to 7.26 (m, 5H), 7.15 to 7.06 (m, 8H), 3.81 (s, 3H); Anal. calcd for  $\text{C}_{31}\text{H}_{22}\text{N}_2\text{O}_3$ : C, 79.15; H, 4.68; N, 5.96. Found: C, 79.21; H, 4.57; N, 5.72.

2) 4-(2-naphthylphenylamine)-N-(2-methoxyphenyl)-1, 8-naphthalimide DMN-2

Mp: 217 to 218 °C; IR (KBr,  $\text{cm}^{-1}$ ): 2 890, 1 689, 1 651, 1 261, 1 234, 758;  $^1\text{H-NMR}$  (300 MHz,  $\text{CDCl}_3$ , TMS,  $\delta$ ): 8.67 (d,  $J = 7.3$  Hz, 1H), 8.58 (d,  $J = 6.2$  Hz, 1H), 8.29 (d,  $J = 8.2$  Hz, 1H), 7.83 to 7.77 (m, 2H), 7.59 to 7.54 (m, 3H), 7.51 (t, 2H), 7.39 to 7.34 (m, 2H), 7.31 to 7.27 (m, 6H), 7.15 to 7.09 (m, 3H), 3.82 (s, 3H); Anal. calcd for  $\text{C}_{35}\text{H}_{24}\text{N}_2\text{O}_3$ : C, 80.77; H, 4.62; N, 5.38. Found: C, 80.42; H, 4.58; N, 5.42.

## 2 Results and Discussion

### 2.1 Synthesis of 1,8-naphthalimide derivatives

The route to the synthesis of 1,8-naphthalimide derivatives DMN-(1-2) is presented in Fig. 1. The starting 4-Br-N-

(2-methoxyphenyl)-1,8-naphthalimide is synthesized according to methods previously described<sup>[11]</sup>. 4-Br-1,8-naphthalic anhydride in a 1:1 molar ratio with aniline is heated under reflux for 12 h in ethanol as a solvent, giving 4-Br-N-(2-methoxyphenyl)-1,8-naphthalimide in good yield (80% to 85%).

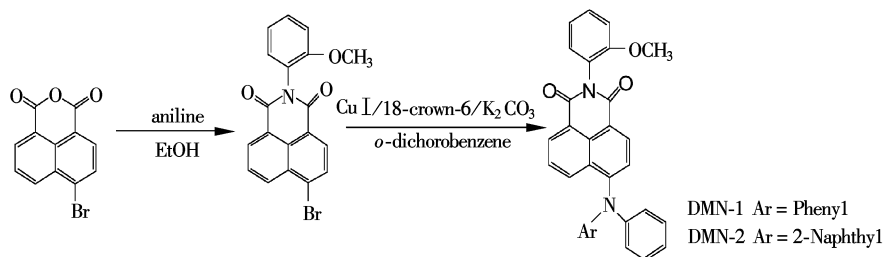


Fig. 1 The synthesis routes of the compounds

The target 1,8-naphthalimide derivatives DMN-(1-2) are obtained by nucleophilic substitution of the bromide atom at C-4 position in 4-Br-N-(2-methoxyphenyl)-1,8-naphthalimide with diarylamine group by reaction with diphenylamine, naphthylphenylamine under copper-catalyzed condition, respectively. One of the most widely used methods for aryl C—N bond construction is the Ullmann condensation, in which a diarylamine is condensed with an aryl halide in the presence of a base and a copper catalyst<sup>[12]</sup>. It is found that the use of crown ethers as phase-transfer catalysts induces rate accelerations and improves yields in certain Ullmann condensation methods<sup>[13]</sup>. Using a standard set of reaction conditions (CuI/18-crown-6/ $K_2CO_3$ /*o*-dichlorobenzene, 190 °C), we couple an array of diarylamines with aryl bromides and obtain the desired pure product in a 25% to 35% yield. Various parameters such as catalyst precursors, base, ligands, and solvents are examined but no better results are obtained. All the compounds are fully characterized by NMR, IR, UV-vis, and elemental analyses.

### 2.2 Thermal stability

The thermal properties of the compounds are determined by thermal gravimetric analysis (TGA) and differential scanning calorimetry (DSC) under a nitrogen atmosphere at a heating rate of 10 °C/min. Fig. 2 shows that the compounds lose less than 5% of their weight on heating to 310, 322 °C respectively, demonstrating their good thermal stability. No glass transition temperature is observed in the heating or cooling cycles in the range of 0 to 250 °C. Starburst molecules having a triarylamine core have demonstrated improved thermal stability. Such an outcome may be due to the asymmetry inherent in these compounds which prevent these low molecular mass compounds from crystallizing.

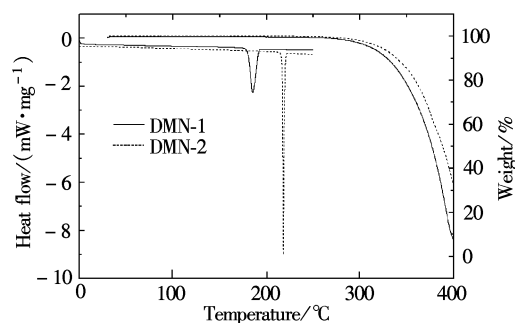


Fig. 2 TGA traces and DSC thermograms of DMN-1 and DMN-2

### 2.3 Photophysical properties

The UV-vis absorption and photoluminescent (PL) spectra of the systems in *n*-hexane, THF and  $CH_2Cl_2$  are recorded to study their spectral properties under various solvent polarities and to compare their emissions with each other. The wavelengths corresponding to the spectral peaks are collected in Tab. 1. A few representative spectra are shown in Fig. 3 and Fig. 4. As indicated in the absorption spectra, these derivatives reveal a common low-energy broad band at 430 to 460 nm assigned to an intramolecular charge-transfer band from the arylamine group to the naphthalimide ring system in *n*-hexane, THF, and  $CH_2Cl_2$ <sup>[14]</sup>. As is typical of a charge-transfer transition, an increase in the polarity of the medium leads to a Stokes shift in the absorption maximum. A change in the solvent from *n*-hexane to  $CH_2Cl_2$  results in an approximate 20 nm bathochromic shift in the absorption maximum of the systems. The magnitude of this shift suggests that the ground state of the molecules is significantly polarized.

Tab. 1 Spectral and photophysical data of DMN-(1-2) in different solvents

Compounds	Solvent	$\Delta f/E_T(30)$	$\lambda_{max}^{abs}/nm$	$\nu_{max}/cm^{-1}$	$\lambda_{max}^{PL}/nm$	$\nu_f/cm^{-1}$	$\Delta\nu/cm^{-1}$
DMN-1	<i>n</i> -hexane	0.001/30.9	438	22 831	492	20 325	2 506
	THF	0.207/37.4	446	22 422	580	17 241	5 181
	$CH_2Cl_2$	0.001/30.9	457	21 882	600	16 667	5 215
DMN-2	<i>n</i> -hexane	0.001/30.9	445	22 472	501	19 960	2 512
	THF	0.207/37.4	452	22 124	598	16 722	5 402
	$CH_2Cl_2$	0.001/30.9	464	21 552	620	16 129	5 423

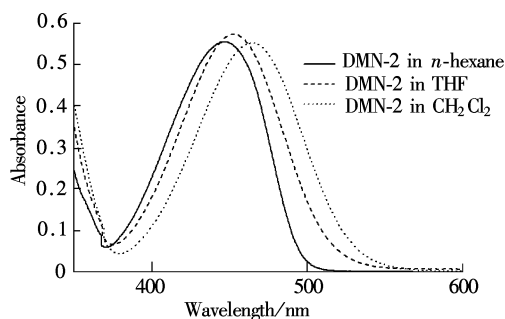


**Fig. 3** Absorption spectra of DMN-2 in *n*-hexane, THF and  $\text{CH}_2\text{Cl}_2$

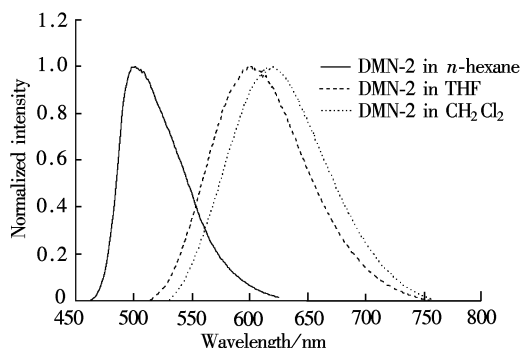


**Fig. 4** Normalized PL spectra of DMN-2 in *n*-hexane, THF and  $\text{CH}_2\text{Cl}_2$

Photoluminescent spectra of the systems are recorded in various solvents with different polarities. The photoluminescent spectra of the systems consist of one broad band except in *n*-hexane, where some structure can be observed. An increase in the polarity of the medium leads to a Stokes shift in the photoluminescent maximum. The effect of the polarity of the medium on the photoluminescent maximum is more pronounced than that on the absorption maximum. This is evident from the data presented in Tab. 1. While a change of the solvent from *n*-hexane to  $\text{CH}_2\text{Cl}_2$  leads to a shift in the absorption maximum of a given system by around 20 nm, the magnitude of the spectral shift is a fifth as large in photoluminescent spectra. This observation suggests that the emitting state of the systems is more polar than the ground state.

The solvent dependence of the fluorescence indicates that the excited state is stabilized in more polar solvents, as expected for an ICT. To obtain more information about the change in the dipole moment upon excitation, we use the Lippert-Mataga equation, Eq. (1), which expresses the Stokes shift as a function of the solvent polarity parameter  $\Delta f(\epsilon, n)$ .

$$v_a - v_f = \frac{2\Delta\mu^2}{hca^3} \Delta f(\epsilon, n) + C = 10\,070 \frac{\Delta\mu^2}{a^3} \Delta f(\epsilon, n) + C \quad (1)$$

and  $\Delta f(\epsilon, n)$  is calculated by

$$\Delta f(\epsilon, n) = \frac{\epsilon - 1}{2\epsilon + 1} - \frac{n^2 - 1}{2n^2 + 1} \quad (2)$$

where  $v_a - v_f$  represents the Stokes shift ( $\text{cm}^{-1}$ );  $v_a$  and  $v_f$

are the spectral positions of the absorption maximum and solvent-equilibrated fluorescent maximum, respectively.  $\Delta\mu$  is given by  $\mu_e - \mu_g$ , which is the magnitude of the change in the dipole moment from the ground state to the excited state. The other terms are as follows:  $h$  corresponds to Plank's constant ( $6.6 \times 10^{-34}$  JS),  $c$  is the velocity of light in the vacuum ( $3.0 \times 10^8$  m/s), and  $a$  is the Onsager cavity radius (m). Onsager cavity radius is estimated from the optimized distance between the two farthest atoms in the direction of charge separation within the molecules, and the Onsager cavity radius  $a$  is set to 0.507 and 0.508 nm, as estimated from the crystallographic molecular volumes of DMN-1 and DMN-2, projected onto a sphere of the same volume.  $\Delta f$  is the orientation polarizability parameter of the solvent where  $n$  is the refractive index of the medium and  $\epsilon$  is the static dielectric constant of the solvent (both at room temperature). The Lippert-Mataga plots for DMN-1 and DMN-2 are shown in Fig. 5. From the slope of this plot, the differences in the dipole moment between the excited state and the ground state are estimated to be 9.2 and 9.8 D for DMN-1 and DMN-2, respectively. This large change in the dipole moment upon excitation is typical for photoinduced ICT processes.

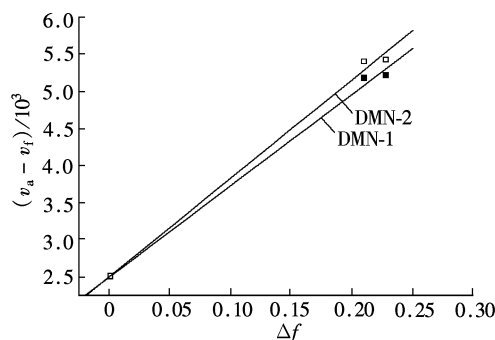


**Fig. 5** Lippert-mataga plot for the DMN-1 and DMN-2

### 3 Conclusion

Two new ICT fluorescence compounds containing 1, 8-naphthalimide derivatives are synthesized in 25% to 35% yields using copper-catalyzed conditions and fully spectroscopically characterized. In addition, the absorption and photoluminescent spectra of these derivatives in *n*-hexane, THF and  $\text{CH}_2\text{Cl}_2$  are investigated. A large Stokes shift in these ICT compounds is observed in polar solvents and the photoluminescent maximum extent to 620 nm in  $\text{CH}_2\text{Cl}_2$ . A change of solvent from *n*-hexane to  $\text{CH}_2\text{Cl}_2$  results in an approximative 20 nm bathochromic shift of the absorption maximum while a fifth as large in photoluminescent spectra.

### References

- [1] Grabchev I, Guittouneau S. Sensors for detecting metal ions and protons based on new green fluorescent poly(amidoamine) dendrimers peripherally modified with 1,8-naphthalimide [J]. *J Photochem Photobiol A*, 2006, **179**(1): 28–34.
- [2] McGehee M D, Heeger A J. Semiconducting (conjugated) polymers as materials for solid-state lasers [J]. *Adv Mater*, 2000, **12**(22): 1655–1668.
- [3] Gao Y Q, Marous R A. Theoretical investigation of the directional electron transfer in 4-aminonaphthalimide compounds

- [J]. *J Phys Chem A*, 2002, **106**(10): 1956 – 1960.
- [4] Gan J, Song Q L, Hou X Y, et al. 1, 8-naphthalimides for non-doping OLEDs: the tunable emission color from blue, green to red [J]. *J Photochem Photobiol A*, 2004, **162**(3): 399 – 406.
- [5] Rideout D, Schinazi R, Pauza C D, et al. Transcriptase and suppress human and feline immunodeficiency virus expression in cultured cells [J]. *J Cell Biochem*, 1993, **51**(2): 446 – 457.
- [6] Kolosov D, Adamovich V, Djurovich P, et al. 1, 8-naphthalimides in phosphorescent organic LEDs: the interplay between dopant, exciplex, and host emission [J]. *J Am Chem Soc*, 2002, **124**(33): 9945.
- [7] Bailly C, Brana M, Waring M. Sequence selective intercalation of antitumour bis-naphthalimides into DNA, evidence for an approach via the major groove [J]. *Eur J Biochem*, 1996, **240**(1): 195 – 208.
- [8] Martynski T, Mykowska K, Bauman D. Spectral properties of fluorescent dyes in nematic liquid crystals [J]. *J Mol Struct*, 1994, **325**(1): 161 – 167.
- [9] Tian H, He Y J, Chang C P. Synthesis and spectral properties of novel laser copolymers based on modified rhodamine 6G and 1, 8-naphthalimide [J]. *J Mater Chem*, 2000, **10**(2): 2049 – 2055.
- [10] Saha S, Samanta A. Influence of the structure of the amino group and polarity of the medium on the photophysical behavior of 4-amino-1, 8-naphthalimide derivatives [J]. *J Phys Chem A*, 2002, **106**(18): 4763 – 4771.
- [11] Alexiou M S, Tychopoulos V, Ghorbanian S, et al. The UV-visible absorption and fluorescence of some substituted 1, 8-naphthalimides and naphthalic anhydrides [J]. *J Chem Soc Perkin Trans*, 1990, **2**(1): 837 – 842.
- [12] Rommens J, van der Auweraer M, de Schryver F C. Hole injection into molecular dispersions of 5'-[4-[Bis(4-ethylphenyl) amino] phenyl]-N, N, N', N'-tetrakis(4-ethylphenyl)-[1, 1': 3', 1''-terphenyl]-4, 4''-diamine [J]. *J Phys Chem B*, 1997, **101**(16): 3081 – 3086.
- [13] Xu Z C, Qian X H, Cui J N. Exploiting the deprotonation mechanism for the design of ratiometric and colorimetric  $Zn^{2+}$  fluorescent chemosensor with a large red-shift in emission [J]. *Tetrahedron*, 2006, **62**(23): 10117 – 10122.
- [14] Islam A, Cheng C C, Cheng C H. Aminonaphthalic anhydrides as red-emitting materials: electroluminescence, crystal structure, and photophysical properties [J]. *J Phys Chem B*, 2005, **109**(12): 5509 – 5517.

## 具有分子内电荷转移特性的 新型萘酰亚胺衍生物合成及发光性能

蒋 伟 唐霖楠 孙岳明 徐文连 王华林

(东南大学化学化工学院, 南京 211189)

**摘要:**以二芳胺和4-溴-1,8-萘酰亚胺体系为原料,经  $CuI/18\text{-crown-6}/K_2CO_3$  催化制备了2个新的萘酰亚胺衍生物,利用 FT-IR, NMR, EA 等表征了其结构.并用 UV-vis 和 PL 测定了此类化合物在正己烷、四氢呋喃和二氯甲烷不同极性溶剂中的发光性能.在 450 nm 附近的紫外最大吸收波长是由于分子内的电荷转移造成的,并且其发射波长在非极性溶剂正己烷中分别位于 492 和 501 nm,而在极性溶剂二氯甲烷中分别位于 600 和 620 nm.采用 Lippert-Mataga 方程计算出分子 4-二苯胺基-N-(2-甲氧基苯基)-1,8-萘酰亚胺(DMN-1)和 4-(2-萘基苯基胺基)-N-(2-甲氧基苯基)-1,8-萘酰亚胺(DMN-2)基态与激发态偶极矩差值分别为 9.2 和 9.8 D,如此大的偶极矩变化说明了该分子具有典型的分子内电荷转移特性.

**关键词:**萘酰亚胺;二芳胺;光致发光;紫外光谱;分子内电荷转移

**中图分类号:**O625